Review

Application of LC-ESI-MS/MS in the analysis of lipid species in samples from patients with X-linked adrenoleukodystrophy, a peroxisomal disease

Kotaro Hama, Yuko Fujiwara, Kazuaki Yokoyama*

Faculty of Pharma-Sciences, Teikyo University, 2−11−1 Kaga, Itabashi-ku, Tokyo 173−8605, Japan

Abstract Peroxisomes are subcellular organelles that are involved in various biological processes, including lipid synthesis and metabolism. Inherited dysfunctions of enzymes in the peroxisome cause a number of peroxisomal disorders associated with unusual lipid metabolites, as exemplified by X-linked adrenoleukodystrophy (X-ALD), the most prevalent peroxisomal disorder. Liquid chromatography linked to electrospray ionization tandem mass spectrometry (LC-ESI-MS/MS) is a pivotal technique for analysis of disease-specific metabolites to facilitate development of diagnostic markers and identification of disease-causing substances. Recent advances in MS have enabled intensive metabolomic targeting of very small amounts of lipids. However, it remains challenging to simultaneously analyze complex lipids such as glycosphingolipids. In addition, it is not easy to obtain stable isotopically labeled compounds for use as internal standards. Here, the application of LC-ESI-MS/MS in the analysis of phospholipids, glycosphingolipids (gangliosides, hexosylceramides, lactosylceramides, and globosides), and fatty acyl-coenzyme A is described. As an example, features of lipid species in X-ALD are described on the basis of the authors' previous studies. A novel method for preparation of deuterated free fatty acids is also introduced, because deuterated compounds are useful as internal standards and probes for enzymes such as lysophospholipid acyltransferases that directly recognize a hydroxyoctadecadienoic acid (HODE) as an oxidized linoleic fatty acid.

Key words: phospholipid, glycosphingolipid, acyl-CoA, X-linked adrenoleukodystrophy, deuterated fatty acid

Abbreviations: ABCD1, ATP-binding cassette subfamily D1; ALD adrenoleukodystrophy; AMN, adrenomyeloneuropathy; acyl-CoA, fatty acyl-coenzyme A; CCALD, childhood cerebral ALD; CE, collision energy; DBS, dried blood spot; GSL, glycosphingolipid; HIE, hydrogen-isotope exchange; HODE, hydroxyoctadecadienoic acid; HSCT, hematopoietic stem cell transplantation; LC-ESI-MS/MS, liquid chromatography linked to electrospray ionization tandem mass spectrometry; lysoPC, lysophosphatidylcholine; SRM, selected reaction monitoring; PEX, peroxin; PL, phospholipid; SED, single enzyme deficiency; VLCFA, very long-chain fatty acid; X-ALD, X-linked ALD

Introduction

Peroxisomes are involved in biological processes such as hydrogen peroxide degradation and glyoxylic acid detoxification. A series of enzymes in peroxisomes is crucial for β-oxidation of saturated or monounsaturated very long-chain fatty acids (VLCFAs), α-oxidation of phytanic acid, and synthesis of plasmalogen, polyunsaturated fatty acids, and bile acids[1]. Peroxisomal disorders are genetic disorders caused by peroxisome dysfunction. The genes responsible for around 30 kinds of peroxisomal disorder have been identified, although the causal relationships between aberrant metabolism due to dysfunctions of the genes and clinical symptoms are still unclear in many of the disorders[2]. Therefore, it is critically important to identify the causative molecules and/or metabolic machinery that explain the pathophysiology, which will also contribute to the develop-

* **Corresponding author**
Kazuaki Yokoyama
Faculty of Pharma-Sciences, Teikyo University, 2−11−1 Kaga, Itabashi-ku, Tokyo 173−8605, Japan
E-mail: yokoyama@pharm.teikyo-u.ac.jp
Received: August 22, 2022. Accepted: October 5, 2022.
Epub November 15, 2022.
DOI: 10.24508/mms.2022.11.006

ment of diagnostic and therapeutic strategies for each peroxisomal disorder. Most peroxisomal disorders display specific lipid profiles that reflect the abnormal metabolic or synthetic processes of lipids in peroxisomes[3,4]. Thus, lipid analysis represents an accurate and rapid diagnostic approach to identifying peroxisomal disorders.

Liquid chromatography linked to electrospray ionization tandem mass spectrometry (LC-ESI-MS/MS) enables structural and quantitative analysis of a number of molecules according to their mass-to-charge ratios (*m/z*) as well as analysis of their physicochemical properties such as hydrophobicity and molecular shape. In this review, the contribution of LC-ESI-MS/MS to research into, and diagnosis of, peroxisomal disorders is briefly described. Technical issues are also discussed in LC-ESI-MS/MS that the authors have worked on for the analysis of X-linked adrenoleukodystrophy (X-ALD), the most prevalent peroxisomal disorder.

Pathology of Peroxisomal Disorders

Peroxisomal disorders are primarily classified into two categories: peroxisome biogenesis disorders, mainly caused by mutations in peroxin (*PEX*) genes that are essential for the assembly of peroxisomes (Table 1), and single enzyme deficiencies (SEDs) caused by defects in enzymes that are located and function in the peroxisome (Table 2)[2]. New peroxisomal disorders are still being identified by whole-genome sequencing analysis.

X-ALD, a representative SED, is caused by dysfunction of ATP-binding cassette subfamily D1 (ABCD1). ABCD1 is located in the peroxisomal membrane and transports VLCFAs with ≥approximately 22 carbons from the cytosol into the peroxisome, which leads to the degradation of these VLCFAs by β-oxidation[5–8]. Consistently, patients with X-ALD display an increased level of VLCFAs from birth, and thus VLCFAs have been analyzed for the diagnosis of X-ALD. X-ALD is characterized by various clinical phenotypes that differ between patients and even between siblings with an identical genetic mutation in *ABCD1* gene. According to the severity and the onset period, X-ALD is divided into subtypes, including childhood cerebral ALD (CCALD; the most common and severe phenotype, such as demyelination of the brain at the age of onset between 3 and 10 years), adolescent cerebral ALD, adult cerebral ALD, adrenomyeloneuropathy (AMN; phenotype with a noninflammatory distal axonopathy that develops after puberty), and Addison only type (phenotype with symptoms of adrenal insufficiency between 2 years and adulthood)[2]. Importantly, there is not significant correlation between the rate of accumulation of VLCFAs and clinical severity, which makes it difficult to provide a presymptomatic diagnosis and effective treatment such as hematopoietic stem cell transplantation (HSCT), which is the only curative treatment and can prevent the progression of neurological symptoms[9].

Current Application of MS for the Diagnosis of X-ALD

Given the specific lipid profiles that reflect abnormalities in peroxisomal metabolism and the synthesis processes of lipids, conventional and accurate lipid analyses contribute substantially to the diagnosis of peroxisomal disorders[10]. In particular, prompt diagnosis of X-ALD is essential because early HSCT is crucial for improving the prognosis of X-ALD patients. Traditionally, the analysis of VLCFAs in

Table 1. Classification of peroxisomal biogenesis disorders[2]

Disease	Responsible gene
Zellweger spectrum disorders	*PEX1*, *2*, *3*, *5*, *6*, *10*, *12*, *13*, *14*, *16*, *19*, *26*
RCDP*1 type 1	*PEX7* (type 1)
RCDP*1 type 5	*PEX5-long isoform* (type 5)
Broad phenotypes of PEX gene defects	*PEX1*, *2*, *3*, *6*, *7*, *10*, *12*, *16*
Mulibrey nanism	*TRIM37**3
PEX11β deficiency	*PEX11*β
EMPF1*2	*DNM1L**4
Charcot-Marie-Tooth disease type 4A	*GDAP1**5

*1 RCDP: Rhizomelic chondrodysplasia punctata. *2 EMPF1: Encephalopathy due to defective mitochondrial and peroxisomal fission 1. *3 TRIM37: Tripartite motif containing 37. *4 *DNM1L*: Dominant negative mutations in dynamin 1-like. *5 *GDAP1*: Ganglioside-induced differentiation-associated protein 1.

Table 2. Classification of peroxisomal single enzyme deficiencies[2)]

Disease (responsible gene)	Impaired biological/metabolic process	Substrate/product (function) of enzyme
X-ALD (*ABCD1*)	Peroxisomal β-oxidation of fatty acids	VLCFA-CoA/(transporter)
ACOX1[*1] deficiency (*ACOX1*)	Peroxisomal β-oxidation of fatty acids	VLCFA-CoA/enoyl-CoA
DBP[*2] deficiency (*HSD17B4*[*3])	Peroxisomal β-oxidation of fatty acids	Enoyl-CoA/D-3-hydroxyacyl-CoA
SCPX[*4] deficiency (*SCP2*[*5])	Peroxisomal β-oxidation of fatty acids	3-ketoacyl-CoA/trimethyltridecanoyl-CoA, choloyl-CoA
AMACR[*6] deficiency (*AMACR*)	Peroxisomal β-oxidation of fatty acids	(25*R*)-D/THC-CoA[*20], (2*R*)-pristanoyl-CoA/(25*S*)-D/THC-CoA, (2*S*)-pristanoyl-CoA
ACBD5[*7] deficiency (*ACBD5*)	Peroxisomal β-oxidation of fatty acids	Acyl-CoA/(binding protein)
ACOX2[*8] deficiency (*ACOX2*)	Bile acid synthesis	(25*S*)-D/THC-CoA, (2*S*)-pristanoyl-CoA/enoyl-CoA
PMP70[*9] deficiency (*ABCD3*[*10])	Bile acid synthesis	D/THC-CoA, phytanoyl-CoA, pristanoyl-CoA/(transporter)
BAAT[*11] deficiency (*BAAT*)	Bile acid synthesis	Choloyl-CoA/taurocholate, glycocholate
Refsum disease (*PHYH*[*12])	α-oxidation of fatty acids	Phytanoyl-CoA/pristanoyl-CoA
RCDP type 2 (*GNPAT*[*13])	Ether-phospholipid synthesis	DHAP[*21]/acyl-DHAP
RCDP type 3 (*AGPS*[*14])	Ether-phospholipid synthesis	Acyl-DHAP/alkyl-DHAP
RCDP type 4 (*FAR1*[*15])	Ether-phospholipid synthesis	Acyl-CoA/fatty-alcohol
Acatalasemia (*CAT*[*16])	Hydrogen peroxide metabolism	Hydrogen peroxide/oxygen and water
Hyperoxaluria type1 (*AGXT*[*17])	Glyoxylate metabolism	Glyoxylic acid/glycine
GOX1[*18] deficiency (*HAO1*[*19])	Glyoxylate metabolism	Glycolic acid/glyoxylic acid

[*1] ACOX1: Acyl-CoA oxidase 1. [*2] DBP: D-bifunctional protein. [*3] HSD17B4: Hydroxysteroid 17-beta dehydrogenase 4. [*4] SCPX: Sterol carrier protein X. [*5] SCP2: Sterol carrier protein 2. [*6] AMACR: Alpha-methylacyl-CoA racemase. [*7] ACBD5: Acyl-CoA binding domain containing 5. [*8] ACOX2: Acyl-CoA oxidase 2. [*9] PMP70: Peroxisomal membrane protein 70 kDa. [*10] ABCD3: ATP-binding cassette sub-family D member 3. [*11] BAAT: Bile acid-CoA:amino acid *N*-acyltransferase. [*12] PHYH: Phytanoyl-CoA 2-hydroxylase. [*13] GNPAT: Glyceronephosphate *O*-acyltransferase. [*14] AGPS: Alkylglycerone phosphate synthase. [*15] FAR1: Fatty acyl-CoA reductase 1. [*16] CAT: Catalase. [*17] AGXT: Alanine-glyoxylate and serine-pyruvate aminotransferase. [*18] GOX1: Glycolate oxidase 1. [*19] HAO1: Hydroxyacid oxidase 1. [*20] D/THC: Di- and tri-hydroxycholestanoyl-CoA. [*21] DHAP: Dihydroxyacetone phosphate

samples from X-ALD patients has been performed using gas chromatography-mass spectrometry[11–13)]. More recently, VLCFAs have also been analyzed by LC-ESI-MS/MS[14)]. In these approaches, both esterified and nonesterified fatty acids in a total lipid fraction are transformed into methyl ester forms, and the amount of C26:0 fatty acid and/or the ratio of C26:0 to C22:0 is used for the diagnosis of X-ALD[4)]. C26:0-lysophosphatidylcholine (lysoPC) was also identified as a new marker for the diagnosis of X-ALD[15)]. C26:0-lysoPC is conventionally extracted from dried blood spot (DBS) samples using methanol and directly analyzed by LC-ESI-MS/MS. Thus, the analysis of C26:0-lysoPC in DBS samples is suitable for high-throughput screening of X-ALD[16,17)]. Large-scale screening of newborns for X-ALD is now conducted in the US (24 states and the district of Columbia), the UK, and the Netherlands and has successfully identified novel lineages of X-ALD[18–21)], showing the validity of LC-ESI-MS/MS for presymptom-

atic diagnosis. A newborn screening project targeting X-ALD also started in 2021 in the Tokai Region of Japan, conducted by Prof. Shimozawa of Gifu University[22].

Insight from Endogenous Lipids in Samples from Patients with X-ALD and ABCD1-Deficient Mice

X-ALD is caused by the dysfunction of a single transporter, ABCD1, although the machineries that explain the phenotypic variance are still unclear, and even the causal relationships between the clinical phenotypes and VLCFAs accumulated in X-ALD patients remain elusive. Most VLCFAs in X-ALD patients are not present in the free form but are incorporated into complex lipids such as phospholipids (PLs)[23,24]. Hence, it is important to precisely analyze the endogenous forms of VLCFAs and clarify the abnormal metabolic pathways caused by the dysfunction of ABCD1. The application of LC-ESI-MS/MS-based techniques in the analysis of PLs, glycosphingolipids (GSLs), and fatty acyl-coenzyme A (acyl-CoA)-containing very long-chain fatty acyl moieties is described below.

PLs

Glycerophospholipids consist of a glycerol backbone linked to polar headgroups at the *sn*-3 position and one or two acyl moieties at the *sn*-1 and/or -2 positions. Sphingomyelin contains phosphorylcholine and an acyl-moiety linked to the hydroxy and amino groups of a sphingoid base, respectively. LC-ESI-MS/MS using a reverse phase columns such as an octadecyl (C_{18}) column has been widely applied to intensively analyze a number of glycerophospholipids and sphingomyelin species with different polar head groups and acyl moieties[25,26]. Because of the wide range of hydrophobicities of PL species, samples were homogenized in methanol and total lipid fractions were extracted using chloroform and methanol (Bligh and Dyer method)[27].

Given that the total concentration of PL species harboring very long-chain fatty acyl moieties (VLCFA-PLs) is small, the amount of PL species was first quantified by selected reaction monitoring (SRM, also called multiple reaction monitoring, MRM), which has a high signal-to-noise ratio. Advantageously, because each PL species dissociates into polar head and hydrophobic groups in this SRM analysis, multiple PL species with identical total carbon and double bond numbers in the acyl moieties as well as an identical polar head group can be detected by a single SRM channel in positive ion mode (Fig. 1A). For example, phosphatidylcholine (PC) species containing either C16:0 and C18:1 (PC 16:0−18:1) or C16:1 and C18:0 (PC 16:1−18:0) can both be analyzed by an SRM channel targeting PC 34:1 (Fig. 1B). Note that phosphatidylinositol species, which can be fragile at higher temperatures, were analyzed more sensitively in positive ion mode when the temperature of the ESI source was set to 200°C rather than 300°C, while the sensitivity of other PLs was not significantly influenced by the temperature of the ESI source in the QTRAP4500 MS instrument[28].

After screening PL species that were significantly altered in samples from patients with X-ALD, the acyl moieties of PLs of interest were analyzed by product ion scanning in negative ion mode. MS/MS/MS analysis was performed using a QTRAP4500 MS instrument for product ion scanning because the first and second precursor ions are tandemly selected by quadrupoles (Q) 1 and 3/linear ion trap (LIT), respectively. Then, accumulated second precursor ions are further subjected to collision induced dissociation in Q3/LIT, which improves the signal-to-noise ratio of the product ions (Fig. 1C). The structure of each PL species was determined from the product ions derived from two fatty acyl moieties and at least one lysophospholipid (lysoPL) for glycerophospholipids as well as a fatty acyl-moiety and a demethylated sphingosylphosphorylcholine for sphingomyelins[28,29]. Notably, the positions of each fatty acyl-moiety in the glycerol backbone can also be determined by comparing the spectral intensities of two lysoPL ions produced from precursor ions because the ion corresponding to 1-acyl-lysoPL arising from loss of the acyl-moiety at the *sn*-2 position is more abundant than the ion of 2-acyl-lysoPL arising from loss of the acyl-moiety at the *sn*-1 position (Fig. 1D)[30,31]. As exemplified by PC 26:0/18:1 and PC 26:1/18:0, very long-chain saturated or monounsaturated fatty acyl moieties were exclusively located at the *sn*-1 position in the glycerol backbone in most VLCFA-PL species in X-ALD fibroblasts and *abcd1*-deficient mice[28,32]. These results are consistent with previous reports on fibroblasts from Zellweger spectrum disorder and a fission yeast mutant, in which VLCFAs were abnormally accumulated, indicating a molecular machinery including enzymes that selectively recognize VLCFAs[33,34].

GSLs

GSLs are composed of hydrophilic carbohydrate chains

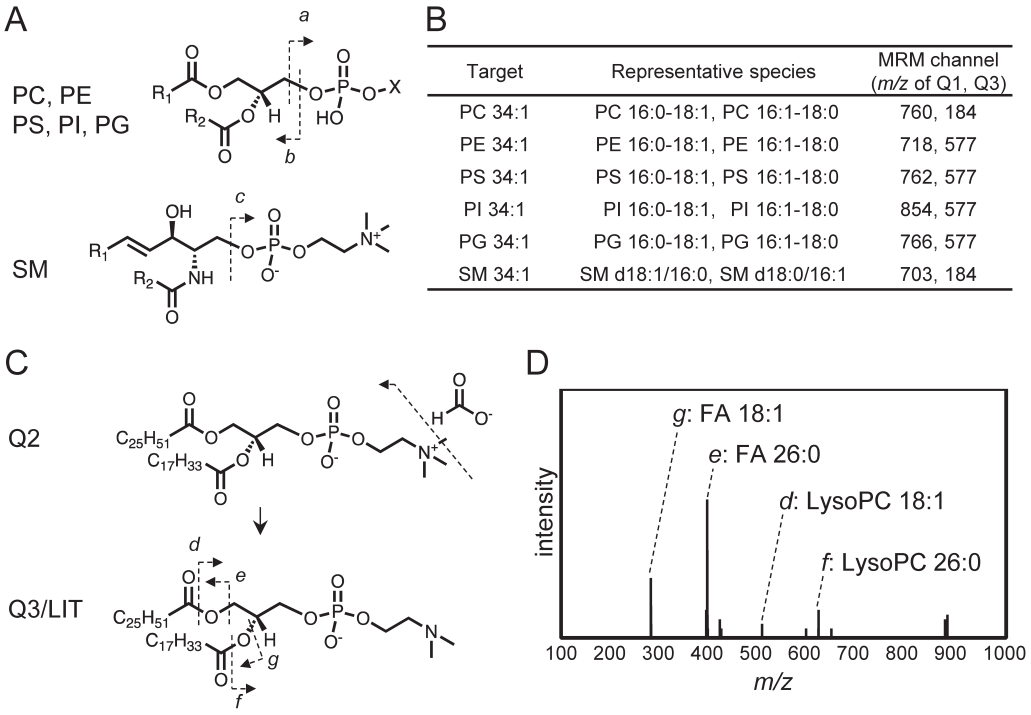

Target	Representative species	MRM channel (*m/z* of Q1, Q3)
PC 34:1	PC 16:0-18:1, PC 16:1-18:0	760, 184
PE 34:1	PE 16:0-18:1, PE 16:1-18:0	718, 577
PS 34:1	PS 16:0-18:1, PS 16:1-18:0	762, 577
PI 34:1	PI 16:0-18:1, PI 16:1-18:0	854, 577
PG 34:1	PG 16:0-18:1, PG 16:1-18:0	766, 577
SM 34:1	SM d18:1/16:0, SM d18:0/16:1	703, 184

Fig. 1. Fragmentation pattern of phospholipids in positive ion mode.

(A) Phospholipid species dissociates into polar head and hydrophobic group in positive ion mode analysis. Generally, protonated phosphorylcholine (*m/z*=184) is mainly observed as the product ion of PC and SM species (marked as ‘*a*’ and ‘*c*’, respectively). In contrast, protonated hydrophobic groups were significant and set as the quadrupole 3 (Q3) value of SRM channel (marked as ‘*b*’). PC: phosphatidylcholine (X=choline); PE: phosphatidylethanolamine (X=ethanolamine); PS: phosphatidylserine (X=serine); PI: phosphatidylinositol (X=inositol); PG: phosphatidylglycerol (X=glycerol); SM: sphingomyelin.

(B) SRM channel settings for detection of a phospholipid molecular species and possible multiple assignments.

Multiple phospholipid species can be analyzed by a single SRM channel according to the total carbon and double bond numbers in each phospholipid.

(C) Product ion of phospholipid in MS/MS/MS of negative ion mode.

The second precursor ion was produced by dissociating a portion of the polar head group of the negatively charged first precursor ion in Q2 and further fragmented into fatty acids (FA) (‘*e*’ and ‘*g*’) and lysophospholipid (‘*d*’ and ‘*f*’) in Q3/linear ion trap (LIT). The lettering corresponds to those in Fig. 1D.

(D) Assignment of product ion spectra. In the case of PC 44:1, four spectra were assigned as two fatty acids and two demethylated lysoPC species. Note that the intensity of the product ion spectrum from lysoPC 26:0 was greater than that from lysoPC 18:1. Thus, the structure of PC 44:1 can be estimated as PC 26:0/18:1 rather than PC 18:1/26:0.

and a hydrophobic ceramide moiety. The metabolism of GSL is associated with the pathogenesis of glycosphingolipidoses and is also implicated in X-ALD (Fig. 2A)[35,36]. Establishing methods that measure each molecular species in GSL classes should aid pathophysiological characterization of GSL species, although the precise analysis of GSL species has been challenging because of the remarkable diversity of GSLs. Separation on the normal phase or hydrophilic interaction chromatography columns that have been used for the analyses of GSLs mainly depends on the sugar moieties of GSLs, and thus GSLs harboring an identical sugar moiety with different ceramide moieties cannot be efficiently separated[37–39]. In contrast, separation on reversed-phase C_{18} columns mainly depends on the ceramide moieties, and thus GSLs harboring an identical ceramide moiety with different carbohydrate chains (e.g., GM1, GM2, and GM3) cannot be easily separated[40].

To help overcome these problems, a novel LC-ESI-MS/MS method using a chiral column (IF-3) that is usually employed for the separation of structural isomers was recently developed[41]. In a series of experiments to optimize the conditions, two parameters of the MS instrument were found to significantly affect the sensitivity of GSL analysis. First, a higher temperature of the ESI ion source resulted in in-source fragmentation of GSLs and decreased sensitivity. For example, in positive ion mode using a QTRAP4500 MS instrument, the signal intensities of three precursor ions of GT1b d18:1/C18:0 with different adducts ($[M+2H]^{2+}$=

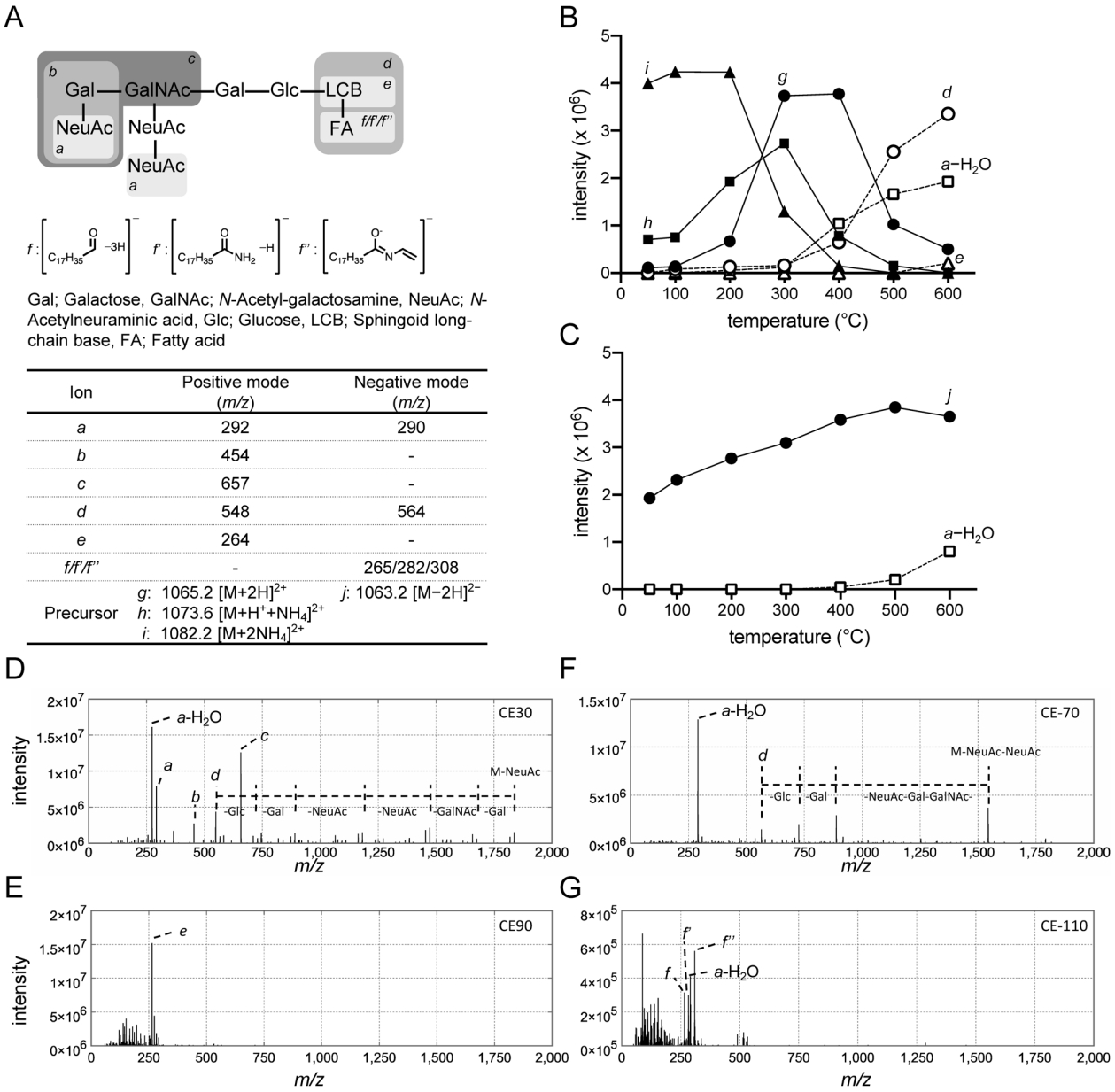

Gal; Galactose, GalNAc; *N*-Acetyl-galactosamine, NeuAc; *N*-Acetylneuraminic acid, Glc; Glucose, LCB; Sphingoid long-chain base, FA; Fatty acid

Ion	Positive mode (*m/z*)	Negative mode (*m/z*)
a	292	290
b	454	-
c	657	-
d	548	564
e	264	-
f/*f*'/*f*''	-	265/282/308
Precursor	*g*: 1065.2 $[M+2H]^{2+}$ *h*: 1073.6 $[M+H^{+}+NH_4]^{2+}$ *i*: 1082.2 $[M+2NH_4]^{2+}$	*j*: 1063.2 $[M-2H]^{2-}$

Fig. 2. Fragmentation patterns and detected ions of GT1b d18:1/C18:0 in LC-MS/MS analysis.

(A) Structure of GT1b. Lettering (*a*–*f*) marking the fragmentation patterns corresponds to the product ions listed in the table in (A) and plot graph in (B–G). The possible structure of fragment ions (*f*/*f*') were indicated according to the previous study[54].

(B, C) Intensity of precursor ions (*g*, *h*, *i*, *j*) and fragment ions (*a*—H_2O, *d*, *e*) of GT1b d18:1/C18:0 at various ESI source temperatures in positive (B) and negative ion mode (C). Both precursor and in-source fragment ions were detected by Q1 scan analysis.

(D–G) Representative patterns of product ions of GT1b d18:1/C18:0 generated through collision induced dissociation. Product ions (*a*/*a*-H_2O, *b*, *c*, *d*, *e*) derived from (*i*; $[M+2NH_4]^{2+}$) at collision energy (CE) of 30 V (D) and 90 V (E) in positive ion mode are marked. Similarly, product ions (*a*-H_2O, *d*, *f*/*f*') from (*j*; $[M-2H]^{2-}$) at CE of −70 V (F) and −110 V (G) in negative ion mode are marked. Both precursor and product ions were analyzed by enhanced product ion scan analysis. *e*: *m/z*=264 was detected with larger CE in all GSLs analyzed.

1065.2, $[M+H+NH_4]^{2+}$=1073.6, and $[M+2NH_4]^{2+}$=1082.2) varied according to the temperature of the ESI, whereas fragment ions of a sialic acid (*m/z*=292), a ceramide moiety (*m/z*=548), and a sphingoid base (*m/z*=264), which were produced by in-source fragmentation, were significant at a higher temperature of the ESI (Fig. 2B). In negative ion mode, by contrast, a precursor ion of GT1b d18:1/C18:0 ($[M-2H]^{2-}$=1063.2) was predominantly detected, while the product ion of a sialic acid (*m/z*=290) was detected even at 600°C with a low (10 V) collision energy (CE) (Fig. 2C).

Second, the CE is crucial in the structural analysis of GSL species. For example, in positive ion mode, structural

information on a ceramide (*m/z*=548), a sialic acid (*m/z*=274/292), and sugar chains (from *m/z*=454 to 1837.7) was efficiently obtained at smaller CE of 30 V (Fig. 2D). In contrast, only a sphingoid long-chain base (*m/z*=264) was efficiently obtained at larger CE of 90 V (Fig. 2E). In negative ion mode, product ions from a sialic acid (*m/z*=290), ceramide (*m/z*=564), and sugar chains were significant at smaller CE of −70 V (Fig. 2F), while a sialic acid (*m/z*=290) and an *N*-fatty acyl-moiety (*m/z*=265/282/308) were significant at larger CE of −110 V (Fig. 2G). Note that using an accurate, high-resolution mass spectrometer, a product ion spectrum from d20:1 sphingosine (calculated exact mass: *m/z*=292.3004) was confirmed to be significant at higher CEs, while those from sialic acid (calculated exact mass: *m/z*=292.1033) were detected at lower CEs in positive ion mode with a Q-Exactive MS instrument. This feature is useful for assigning the structures of GSL species.

Following on from the above experiments and more extensive experiments with GalCer, GlcCer, LacCer, Sulfatide, GM3, GM2, GM1, GD1a, GD3, Gb3, and Gb4, a common fragment ion from d18:1 sphingosine (*m/z*=264) was applied as a product ion in each SRM channel with high CE (>70 V) in positive ion mode. Given that GSL species harboring a d18:1 sphingosine moiety make up the majority of the total GSL fraction, the present method enables simultaneous measurement of a number of GSL species with high sensitivity. Cells were homogenized and deproteinized by methanol, and analytes were measured using the LC-ESI-MS/MS method and applying the chiral column (IF-3) and MS conditions described above. The level of C25- or C26-containing GSL species was found to be elevated in fibroblasts from patients with X-ALD. Notably, C44:1 HexCer (galactosylceramide and/or glucosylceramide) was significantly more accumulated in fibroblasts from patients with severe CCALD than in that with moderate-phenotype AMN, indicating different profiles of GSL species containing VLCFAs between patients with different clinical phenotypes[42]. Further precise analysis of GSL species will aid in discriminating between different X-ALD subtypes.

Acyl-CoA

Acyl-CoA species are amphiphilic metabolites composed of a hydrophilic CoA and a hydrophobic fatty acyl-moiety joined by a thioester linkage. Very long-chain fatty acyl-coenzyme A (VLCFA-CoA) species are endogenously synthesized through the fatty acid elongation process by ELOVL1 and serve as metabolic intermediates of VLCFAs such as in β-oxidation and PL synthesis[43,44]. Thus, it is important to quantify the intracellular pool of each acyl-CoA species to analyze the effect of ABCD1 dysfunction on VLCFA metabolism. However, when using conventional hydrophobic or hydrophilic interaction chromatography, the amphiphilic properties of acyl-CoA hamper the efficient separation of acyl-CoA species. Kasuya and co-workers developed an LC-ESI-MS/MS method using ammonium acetate buffer (pH 5.3) and acetonitrile as the mobile phases and analyzed short-, medium-, and long chain acyl-CoA species[45,46]. Haynes, Merrill and co-workers used triethylamine as an ion-paring reagent in a mobile phase and developed an LC-ESI-MS/MS method to quantify long-chain acyl-CoA species[47]. Recently, acyl-CoA species were found to be efficiently separated by LC-ESI-MS/MS using an octyl column with high sensitivity by adjusting the mobile phases to pH 9.0 with ammonium hydroxide, suggesting that ion-paring reagents or ammonium hydroxide might be crucial to attenuate interactions between acyl-CoA and the HPLC column, such as chelate formation with residual silanol groups and/or metals, for the efficient separation of acyl-CoA species. In the recent study, cells were homogenized in acetonitrile/isopropanol (3 : 1 by volume) and analytes were prepared by solid phase extraction using a 2-(2-pyridyl)ethyl silica gel column. Then acyl-CoA species were precisely analyzed by LC-ESI-MS/MS using deuterated C16:0-d_{31}-CoA chemically synthesized from C16:0-d_{31} free fatty acid (FFA C16:0-d_{31}) as an internal standard (IS) compound. Hexacosenoyl (C26:1)-CoA, rather than hexacosanoyl (C26:0)-CoA, was found to be most abundant among the VLCFA-CoA species in fibroblasts from patients with X-ALD and ABCD1-deficient HeLa cells[32]. In contrast, the amount of FFA C26:0 was larger than the amount of FFA C26:1 in fibroblasts from patients with X-ALD (unpublished results), suggesting that intracellular C26:0-CoA is more efficiently metabolized than C26:1-CoA. Given that chloroquine was recently identified to attenuate abnormal behavior in ABCD1-deficient zebrafish by increasing the expression level of stearoyl-CoA desaturase-1, it would be fascinating to determine whether a metabolic difference between saturated and monounsaturated VLCFA-CoAs is involved in the pathology of X-ALD[48].

Application of Deuterium-labeled Fatty Acids in Lipidomic Analysis

Stable isotopically labeled analogs are desirable as IS compounds because these unnatural compounds can properly compensate for the variation in sample extraction and ionization efficiency of target molecules due to ion suppression/enhancement in LC-ESI-MS/MS analyses[49]. These isotopically labeled analogs are also useful as probes to reveal the metabolic pathways of target molecules because, as unaffected and metabolized forms, they are easily measured separately from endogenous compounds according to the *m/z* difference by LC-ESI-MS/MS, although it is still difficult to prepare corresponding these labeled compounds. To address these difficulties, several hydrogen-isotope exchange (HIE) methods have been reported by which one can chemically synthesize deuterated fatty acids[50]. Very recently, a novel HIE method to synthesize tetradeuterated fatty acids was developed; the free fatty acid of interest is derivatized into 8-amino-quinoline amides, followed by catalytic and K_2CO_3-mediated deuteration at the β- and α-carbons of the fatty acid, respectively (Fig. 3A)[51]. This HIE method can be applied to a variety of fatty acids, including polyunsaturated fatty acids, *cis*/*trans* fatty acids, and hydroxylated fatty acids as starting materials, providing a strategy to prepare IS compounds and probes for metabolic analysis that have previously been difficult to prepare. In particular, the α-deuterium of the tetradeuterated fatty acyl-moiety at the *sn*-2 position of PC was amenable to incorporation into the phosphorylcholine fragment through collision-induced dissociation[52,53], producing a diagnostic phosphorylcholine-d_1 ion at *m/z*=185, which facilitated the analysis of fatty acid metabolism in PC synthesis (Fig. 3B). Indeed, using synthesized tetradeuterated oxidized linoleic acid (HODE-d_4; hydroxyoctadecadienoic acid-d_4) and HODE-d_4-CoA, three enzymes (LPCAT1/LPLAT8, LPCAT2/LPLAT9, and AGPAT7/LPLAT10) were revealed to be acyltransferases that directly transfer HODE-CoA into lysoPC to produce PC species with a hydroxylated fatty acyl-moiety (Fig. 3C)[51]. Given the validity of tetradeuterated fatty acids, it would be possible to precisely dissect the aberrant lipid metabolism caused by *ABCD1* disfunction in X-ALD patients.

Conclusion

To develop diagnostic and therapeutic methods for peroxisomal disorders, it is crucial to identify the causative

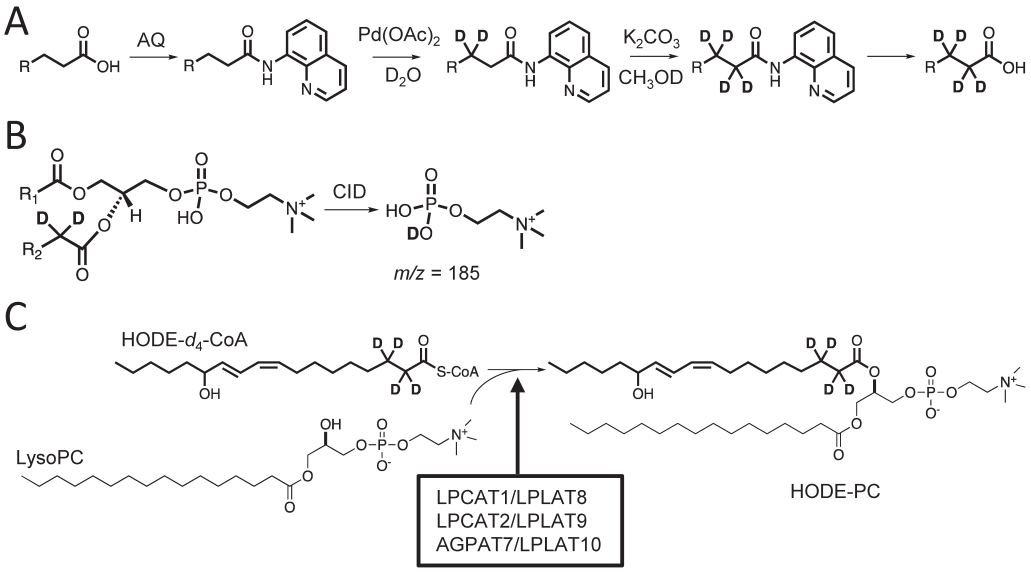

Fig. 3. Synthesis and application of tetradeuterated fatty acid.

(A) Synthesis of tetradeuterated free fatty acid. Fatty acyl amides with 8-amino-quinoline (AQ) were deuterated at the β-carbon of the fatty acyl-moiety by heavy water (D_2O) and palladium catalyst ($Pd(OAc)_2$). Hydrogens at the α-carbon of the amides were further exchanged with deuterium atoms from CH_3OD by K_2CO_3, and tetradeuterated free fatty acids were obtained by hydrolysis.

(B) Production of deuterated phosphorylcholine in collision-induced dissociation (CID). In the process of CID, α-deuterium of the tetradeuterated fatty acyl-moiety at the *sn*-2 position of PC was incorporated into the phosphorylcholine fragment, producing a diagnostic phosphorylcholine-d_1 ion at *m/z*=185.

(C) Identification of acyltransferases that transfer hydroxyoctadecadienoic acid (HODE)-CoA into lysoPC. Three lysophospholipid acyltransferases (LPCAT1/LPLAT8, LPCAT2/LPLAT9 and AGPAT7/LPLAT10) directly recognized a deuterated hydroxylated linoleic fatty acyl-CoA (HODE-d_4-CoA) as a substrate.

molecules and/or metabolic machinery that explain the pathophysiology. To this end, it is important to precisely analyze the localization as well as the amount of target molecules. Recent imaging MS techniques have enabled direct analysis of VLCFA-PL on the brain section of *Abcd1*-deficient mice[28]. Moreover, it is now even possible to dissect individual structural isomers, such as the position of the double bonds in fatty acid molecules by LC-ESI-MS/MS, although it remains important to optimize the LC and MS conditions to develop sensitive and robust analyses. Progress in LC-ESI-MS/MS supported by persistent optimization will contribute to elucidation of the details of VLCFA metabolism.

Conflict of Interest

The authors declare that they have no conflict of interest.

Informed Consent and Animal Welfare

This study abides by the Declaration of Helsinki Principles, and the research protocol was approved by the Teikyo University Ethical Review Board for Medical and Health Research Involving Human Subjects (#20-075). Written informed consent was obtained from all participants. All procedures performed in studies involving animals were in accordance with the ethical standards of the University Committee for Animal Use and Care in Teikyo University (#12-050).

Acknowledgments

We thank Profs. Shigeo Takashima and Nobuyuki Shimozawa (Gifu University) for providing samples from patients with X-ALD, and Profs. Masashi Morita (Toyama University) and Tsuneo Imanaka (Hiroshima International University) for samples from *Abcd1*-deficient mice. We also thank Dr. Ayako Watanabe (University of Tokyo) and Prof. Ryo Takita (University of Shizuoka) for synthesizing the tetradeuterated fatty acids, and Atsushi Yamashita (Teikyo University) for technical advice in acyl-CoA synthesis. We thank Prof. Mitsutoshi Setou (Hamamatsu University School of Medicine) for the analysis using imaging mass spectrometry. We thank Prof. Hideyo Takahashi (Tokyo University of Science) for the helpful discussion. Finally, we thank Ms. Kumiko Kurosaki and colleagues (Central Laboratory of Teikyo University) for supporting the analysis using LC-ESI-MS/MS.

References

1) Morita M, Imanaka T: The function of the peroxisome, in Imanaka T, Shimozawa N (eds): *Peroxisomes: Biogenesis*, *function*, *and role in human disease.* p. 59−104, Springer Singapore, Singapore, 2019.
2) Shimozawa N: Peroxisomal disorders, in Imanaka T, Shimozawa N (eds): *Peroxisomes: Biogenesis*, *function*, *and role in human disease.* p. 107−136, Springer Singapore, Singapore, 2019.
3) Wanders RJA: Peroxisomal disorders: Improved laboratory diagnosis, new defects and the complicated route to treatment. *Mol Cell Probes* 40: 60−69, 2018.
4) Shimozawa N. Diagnosis of peroxisomal disorders, in Imanaka T, Shimozawa N (eds): *Peroxisomes: Biogenesis*, *function*, *and role in human disease.* p. 159−169, Springer Singapore, Singapore, 2019.
5) Mosser J, Douar AM, Sarde CO, Kioschis P, Feil R, et al: Putative X-linked adrenoleukodystrophy gene shares unexpected homology with ABC transporters. *Nature* 361: 726−730, 1993.
6) van Roermund CW, Visser WF, Ijlst L, Waterham HR, Wanders RJ: Differential substrate specificities of human ABCD1 and ABCD2 in peroxisomal fatty acid β-oxidation. *Biochim Biophys Acta* 1811: 148−152, 2011.
7) Wiesinger C, Kunze M, Regelsberger G, Forss-Petter S, Berger J: Impaired very long-chain acyl-CoA β-oxidation in human X-linked adrenoleukodystrophy fibroblasts is a direct consequence of ABCD1 transporter dysfunction. *J Biol Chem 288*: 19269−19279, 2013.
8) Chen ZP, Xu D, Wang L, Mao YX, Li Y, et al: Structural basis of substrate recognition and translocation by human very long-chain fatty acid transporter ABCD1. *Nat Commun* 3299, DOI:10.1038/s41467-022-30974-5, 2022.
9) Mahmood A, Raymond GV, Dubey P, Peters C, Moser HW: Survival analysis of haematopoietic cell transplantation for childhood cerebral X-linked adrenoleukodystrophy: A comparison study. *Lancet Neurol* 6: 687−692, 2007.
10) Hama K, Fujiwara Y, Yokoyama K: Lipidomics of peroxisomal disorders, in Imanaka T, Shimozawa N (eds): *Peroxisomes: Biogenesis*, *function*, *and role in human disease.* p. 249−260, Springer Singapore, Singapore, 2019.
11) Martinez M, Mougan I, Roig M, Ballabriga A: Blood polyunsaturated fatty acids in patients with peroxisomal disorders. A multicenter study. *Lipids* 29: 273−280, 1994.
12) Moser AB, Jones DS, Raymond GV, Moser HW: Plasma and red blood cell fatty acids in peroxisomal disorders.

Neurochem Res 24: 187−197, 1999.

13) Takemoto Y, Suzuki Y, Horibe R, Shimozawa N, Wanders RJ, et al: Gas chromatography/mass spectrometry analysis of very long chain fatty acids, docosahexaenoic acid, phytanic acid and plasmalogen for the screening of peroxisomal disorders. *Brain Dev* 25: 481−487, 2003.
14) Takashima S, Toyoshi K, Itoh T, Kajiwara N, Honda A, et al: Detection of unusual very-long-chain fatty acid and ether lipid derivatives in the fibroblasts and plasma of patients with peroxisomal diseases using liquid chromatography-mass spectrometry. *Mol Genet Metab* 120: 255−268, 2017.
15) Hubbard WC, Moser AB, Tortorelli S, Liu A, Jones D, et al: Combined liquid chromatography-tandem mass spectrometry as an analytical method for high throughput screening for X-linked adrenoleukodystrophy and other peroxisomal disorders: preliminary findings. *Mol Genet Metab* 89:185−187, 2006.
16) Hubbard WC, Moser AB, Liu AC, Jones RO, Steinberg SJ, et al: Newborn screening for X-linked adrenoleukodystrophy (X-ALD): Validation of a combined liquid chromatography-tandem mass spectrometric (LC-MS/MS) method. *Mol. Genet Metab* 97: 212−220, 2009.
17) Theda C, Gibbons K, Defor TE, Donohue PK, Golden WC, et al: Newborn screening for X-linked adrenoleukodystrophy: Further evidence high throughput screening is feasible. *Mol Genet Metab* 111: 55−57, 2014.
18) Moser AB, Seeger E, Raymond GV. Newborn screening for X-linked adrenoleukodystrophy: Past, present, and future. *Int J Neonatal Screen* 8: 16, DOI:10.3390/ijns 8010016, 2022.
19) Bessey A, Chilcott JB, Leaviss J, Sutton A: Economic impact of screening for X-linked Adrenoleukodystrophy within a newborn blood spot screening programme. *Orphanet J Rare Dis* 13:179, DOI:10.1186/s13023-018-0921-4, 2018.
20) Barendsen RW, Dijkstra IME, Visser WF, Alders M, Bliek J, et al: Adrenoleukodystrophy newborn screening in the Netherlands (SCAN Study): The X-factor. *Front Cell Dev Biol* 8:499, DOI:10.3389/fcell.2020.00499, 2020.
21) Vogel BH, Bradley SE, Adams DJ, D'Aco K, Erbe RW, et al: Newborn screening for X-linked adrenoleukodystrophy in New York State: Diagnostic protocol, surveillance protocol and treatment guidelines. *Mol Genet Metab* 114: 599−603, 2015.
22) Shimozawa N, Takashima S, Kawai H, Kubota K, Sasai H, et al: Advanced diagnostic system and introduction of newborn screening of adrenoleukodystrophy and peroxisomal disorders in Japan. *Int J Neonatal Screen* 7: 58, DOI:10.3390/ijns7030058, 2021.
23) Moser HW SK, Watkins PA, Powers J, Moser AB: X-linked adrenoleukodystrophy, in Scriver CR BA, Sly WS, Valle D (eds): *The metabolic and molecular bases of inherited disease. 8th ed.* Vol 2. p. 3257−3301, McGraw-Hill, New York, 2001.
24) Abe Y, Honsho M, Nakanishi H, Taguchi R, Fujiki Y: Very-long-chain polyunsaturated fatty acids accumulate in phosphatidylcholine of fibroblasts from patients with Zellweger syndrome and acyl-CoA oxidase1 deficiency. *Biochim Biophys Acta* 1841: 610−619, 2014.
25) Haroldsen PE, Murphy RC: Analysis of phospholipid molecular species in rat lung as dinitrobenzoate diglycerides by electron capture negative chemical ionization mass spectrometry. *Biomed Environ Mass Spectrom* 14: 573−578, 1987.
26) Taguchi R, Houjou T, Nakanishi H, Yamazaki T, Ishida M, et al: Focused lipidomics by tandem mass spectrometry. *J Chromatogr B Analyt Technol Biomed Life Sci* 823: 26−36, 2005.
27) Bligh EG, Dyer WJ: A rapid method of total lipid extraction and purification. *Can J Biochem Physiol* 37: 911−917, 1959.
28) Hama K, Fujiwara Y, Morita M, Yamazaki F, Nakashima Y, et al: Profiling and imaging of phospholipids in brains of *Abcd1*-Deficient mice. *Lipids* 53: 85−102, 2018.
29) Hama K, Fujiwara Y, Tabata H, Takahashi H, Yokoyama K: Comprehensive quantitation using two stable isotopically labeled species and direct detection of *N*-acyl moiety of sphingomyelin. *Lipids* 52: 789−799, 2017.
30) Hsu FF, Turk J: Electrospray ionization with low-energy collisionally activated dissociation tandem mass spectrometry of glycerophospholipids: Mechanisms of fragmentation and structural characterization. *J Chromatogr* 877: 2673−2695, 2009.
31) Nakanishi H, Iida Y, Shimizu T, Taguchi R: Separation and quantification of sn-1 and *sn*-2 fatty acid positional isomers in phosphatidylcholine by RPLC-ESI MS/MS. *J Biochem* 147: 245−256, 2010.
32) Hama K, Fujiwara Y, Takashima S, Hayashi Y, Yamashita A, et al: Hexacosenoyl-CoA is the most abundant very long-chain acyl-CoA in ATP binding cassette transporter D1-deficient cells. *J Lipid Res* 61: 523−536, 2020.

33) Hama K, Nagai T, Nishizawa C, Ikeda K, Morita M, et al: Molecular species of phospholipids with very long chain fatty acids in skin fibroblasts of Zellweger syndrome. *Lipids* 48: 1253−1267, 2013.

34) Yokoyama K, Saitoh S, Ishida M, Yamakawa Y, Nakamura K, et al: Very-long-chain fatty acid-containing phospholipids accumulate in fatty acid synthase temperature-sensitive mutant strains of the fission yeast Schizosaccharomyces pombe fas2/lsd1. *Biochim Biophys Acta* 1532: 223−233, 2001.

35) Annunziata I, Sano R, d'Azzo A: Mitochondria-associated ER membranes (MAMs) and lysosomal storage diseases. *Cell Death Dis.* 9: 328, DOI:10.1038/s41419-017-0025-4, 2018.

36) Igarashi M, Belchis D, Suzuki K: Brain gangliosides in adrenoleukodystrophy. *J Neurochem* 27: 327−328, 1976.

37) Wagener R, Kobbe B, Stoffel W: Quantification of gangliosides by microbore high performance liquid chromatography. *J Lipid Res* 37: 1823−1829, 1996.

38) Scherer M, Leuthäuser-Jaschinski K, Ecker J, Schmitz G, Liebisch G: A rapid and quantitative LC-MS/MS method to profile sphingolipids. *J Lipid Res* 51: 2001−2011, 2010.

39) Ikeda K, Taguchi R: Highly sensitive localization analysis of gangliosides and sulfatides including structural isomers in mouse cerebellum sections by combination of laser microdissection and hydrophilic interaction liquid chromatography/electrospray ionization mass spectrometry with theoretically expanded multiple reaction monitoring. *Rapid Commun Mass Spectrom* 24: 2957−2965, 2010.

40) Ikeda K, Shimizu T, Taguchi R: Targeted analysis of ganglioside and sulfatide molecular species by LC/ESI-MS/MS with theoretically expanded multiple reaction monitoring. *J Lipid Res* 49: 2678−2689, 2008.

41) Fujiwara Y, Hama K, Yokoyama K: Mass spectrometry in combination with a chiral column and multichannel-MRM allows comprehensive analysis of glycosphingolipid molecular species from mouse brain. *Carbohydr Res* 490:107959, DOI:10.1016/j.carres.2020.107959, 2020.

42) Fujiwara Y, Hama K, Shimozawa N, Yokoyama K: Glycosphingolipids with very long-chain fatty acids accumulate in fibroblasts from adrenoleukodystrophy patients. *Int J Mol Sci* 22, DOI:10.3390/ijns22168645, 2021.

43) Tsuji S, Ohno T, Miyatake T, Suzuki A, Yamakawa T: Fatty acid elongation activity in fibroblasts from patients with adrenoleukodystrophy (ALD). *J Biochem* 96: 1241−1247, 1984.

44) Ofman R, Dijkstra IM, van Roermund CW, Burger N, Turkenburg M, et al: The role of ELOVL1 in very long-chain fatty acid homeostasis and X-linked adrenoleukodystrophy. *EMBO Mol Med* 2: 90−97, 2010.

45) Kasuya F, Oti Y, Tatsuki T, Igarashi K: Analysis of medium-chain acyl-coenzyme A esters in mouse tissues by liquid chromatography-electrospray ionization mass spectrometry. *Anal Biochem* 325: 196−205, 2004.

46) Kasuya F, Masuyama T, Yamashita T, Nakamoto K, Tokuyama S, Kawakami H: Determination of acyl-CoA esters and acyl-CoA synthetase activity in mouse brain areas by liquid chromatography-electrospray ionization-tandem mass spectrometry. *J Chromatogr* 929: 45−50, 2013.

47) Haynes CA, Allegood JC, Sims K, Wang EW, Sullards MC, et al: Quantitation of fatty acyl-coenzyme As in mammalian cells by liquid chromatography-electrospray ionization tandem mass spectrometry. *J Lipid Res* 49: 1113−1125, 2008.

48) Raas Q, van de Beek MC, Forss-Petter S, et al: Metabolic rerouting via SCD1 induction impacts X-linked adrenoleukodystrophy. *J Clin Invest* 131, DOI:10.1172/JCI142500, 2021.

49) Burla B, Arita M, Arita M, et al: MS-based lipidomics of human blood plasma: A community-initiated position paper to develop accepted guidelines. *J Lipid Res* 59: 2001−2017, 2018.

50) Kopf S, Bourriquen F, Li W, Neumann H, Junge K, et al: Recent developments for the deuterium and tritium labeling of organic molecules. *Chem Rev* 122: 6634−6718, 2022.

51) Watanabe A, Hama K, Watanabe K, Fujiwara Y, Yokoyama K, et al: Controlled tetradeuteration of straight-chain fatty acids: Synthesis, Application, and insight into the metabolism of oxidized linoleic acid. *Angew Chem Int Ed Engl* 61: e202202779, DOI:10.1002/anie.202202779, 2022.

52) Hsu FF, Turk J: Electrospray ionization/tandem quadrupole mass spectrometric studies on phosphatidylcholines: The fragmentation processes. *J Am Soc Mass Spectrom* 14: 352−363, 2003.

53) Kirschbaum C, Greis K, Polewski L, Gewinner S, Schöllkopf W, et al: Unveiling glycerolipid fragmentation by cryogenic infrared spectroscopy. *J Am Chem Soc* 143: 14827−14834, 2021.

54) Tsugawa H, Ikeda K, Tanaka W, Senoo Y, Arita M, et al: Comprehensive identification of sphingolipid species by in silico retention time and tandem mass spectral library. *J Cheminform* 9: DOI: 10.1186/s13321-017-0205-3, 2017.